Jordan Journal of Civil Engineering, Volume **4**, No. **2**, **2010**

Symmetrical and Anti-Symmetrical Buckling of Long Corroded Cylindrical Shell Subjected to External Pressure

Anis S. Shatnawi [1)], ***Samir Z. Al-Sadder*** [2)], ***Mutasim S. Abdel-Jaber*** [1)] ***and Robert Beale*** [3)]

[1)] Department of Civil Engineering, Faculty of Engineering, The University of Jordan, Amman 11942, Jordan
Corresponding Author. Tel.: +962 6 5355000 x.21139; fax: +962 6 5355588,
E-mail: ashatnawi@ju.edu.jo (Anis S. Shatnawi)
[2)] Department of Civil Engineering, Faculty of Engineering, Hashemite University, Zarka 13115, Jordan
[3)] Department of Mechanical Engineering, School of Technology,Oxford Brookes University, UK. OX33 1HX

ABSTRACT

This paper derives an exact analytical solution for determining elastic critical buckling pressures and mode shapes for very long corroded cylindrical steel shells subjected to external pressure considering symmetrical and anti-symmetrical mode cases. The corroded long cylindrical shell has been modelled as a non-uniform "stepped-type" ring consisting of two portions- corroded and un-corroded regions. A full range parametric study has been made to investigate the effect of corrosion angular extent and corrosion thickness on the elastic buckling pressures and their modes. The study shows that buckling loads and modes depend on the corrosion angular extent β and the corroded to un-corroded thicknesses ratio. The results are verified by a set of investigations with a series of corroded cylindrical shells. They showed a close agreement with those obtained from using the finite element package ABAQUS.

KEYWORDS: Buckling, Corroded cylindrical shell, External pressure.

INTRODUCTION

With the recent developments in marine oil exploitation, corrosion in pipelines - which are typically made as very long cylindrical steel shells - has lately become a serious issue concerning the marine environment. In the offshore industry, the pipelines are even laid down over the seabed, where they are exposed to a more corrosive environment. Corrosion will affect the service life of the pipelines and may greatly decrease the structural integrity and lead to a catastrophic failure (Fatt, 1999; Xue and Fatt, 2002).

Solutions of buckling problems for the structural failure of uniform shells and pipelines have been well established (Timoshenko and Gere, 1961; Pinna and Ronalds, 2000; Vodenitcharova and Ansourian, 1996). Due to corrosion in thin shells as pipelines, the thin-walled cross-section of the cylindrical shell will no longer be uniform. Despite much research undertaken into the analysis of uniform cylindrical shells, results of studies into failures of non-uniform cylindrical shells and corroded pipelines are very limited. Earlier attempts to account for corrosion were based on assuming the corrosion to spread around the entire circumference of the cylindrical shell (Bai and Hauch, 1998; Bai et al., 1999). This type of solutions can not explain the influence of the angular extension of the corrosion region on the critical load or predict the anti-symmetrical mode shapes. The importance of capturing the anti-symmetrical mode shapes comes from the fact

Accepted for Publication on 15/4/2010.

that all pipelines are manufactured with imperfections. Such imperfections and corrosions can induce anti-symmetric buckling modes of the non-uniform cylindrical shells (Xue, 2002).

Fatt (1999) and Xue and Fatt (2002) presented an effective model describing the corroded region in terms of the depth and angular extent of corrosion. Their model can capture anti-symmetrical mode shapes with only one stepped region. However, the corroded region in their model was assumed to be symmetric along the circumferential center line which does not represent the true shape of the corroded region in the pipelines. However, it can be used as a benchmark in more advanced studies for unsymmetric corroded regions along the circumferential center line. They further developed (Xue and Fatt, 2005) a rigid plastic model, with again only single stepped region, to obtain an estimate of the ultimate collapse pressure. Both their buckling and collapse models were verified using the computer program ABAQUS (ABAQUS/Standard User's Manual, 2003).

In this paper, an exact analytical solution for determining elastic critical buckling pressures and mode shapes for a very long corroded cylindrical steel shell subjected to external hydrostatic pressure will be carried out. The solution will take into consideration the effect of geometric non-uniformity of thickness and angular extent in both symmetrical and anti-symmetrical mode cases. In this study, the multi stepped type solution has been carried out to enable capturing any corroded curve which may occur. It can follow up many polynomial curves as parabolic, cubic and other polynomials. The solution will be verified by using the finite element package ABAQUS (ABAQUS/Standard User's Manual, 2003) and will be investigated for a series of corroded cylindrical shells. This study shows that buckling loads and modes depends on the corrosion angular extent β and the corroded to un-corroded thicknesses ratio. This study can be used as a benchmark in monitoring buckling propagation in corroded pipelines in many engineering applications such as offshore and oil industries. Moreover, the results of this research can be used as a guide to the analysis of the stability of corroded pipelines against buckling. This paper also presents the results of the bucckling analysis of an unsymmetrical corroded region.

PROBLEM DESCRIPTION

A very long steel pipeline was modeled as a non-uniform cross-section (i.e., stepped-type) cylindrical shell that was divided into two portions; un-corroded and corroded portions. Keeping in mind the symmetry of the problem, and to present the stepped-type non-uniformity of the corroded portion, it was divided to five regions with an equal angular extent β but with subsequent decreasing in thickness. However, the corroded portion of the ring can be divided into any number of regions to capture the actual corrosion in the ring and its buckling loads and modes. The variation of the corroded shell thickness within the corroded region of the ring is assumed to be parabolic. One may keep in mind that this study considers the shell as ideal ring and does not account for the effect of geometrical imperfections on the buckling loads.

Now, let us consider a ring with a nominal radius R and non-uniform stepped thickness as shown in Fig. 1. The thickness reduction was assumed to be symmetric with respect to the centerline of the ring at $\theta = 0$ (i.e., geometrical symmetrical condition). The ring was divided into two portions, first the un-corroded region that is denoted by region 6 having a thickness equal to t_6 and the other portion of the ring has been assumed to be the corroded regions that are regions 5 to 1 which have thicknesses t_5 to t_1, respectively. The ring consisted of six regions with different thicknesses, but with a common neutral axis. The corroded portion was represented by consequent uniform stepped reduction in thicknesses with an equal angular extent equal to β. On the other hand, the un-corroded portion has an angular extent equal to π-5β. The material of the ring was assumed to be linearly elastic with modulus of elasticity E and Poisson's ratio υ. The ring was subjected to an external uniform hydrostatic pressure equal to p.

To simplify the problem, plane elasticity theory was

adopted with a small thickness to mean radius ratio. The ring was modeled as six regions of curved beams that can buckle under external pressure. Both symmetrical and anti-symmetrical buckling modes were individually taken into consideration. The actual buckling pressures and modes of the non-uniform ring are analytically obtained as the smallest value of either the critical buckling pressure of symmetric or anti-symmetric modes.

DERIVATION AND FORMULATION OF THE EIGENVALUE PROBLEM

The differential equations governing the behavior of a thin non-uniform ring subjected to external hydrostatic pressure with the cross-section shown in Fig. 1 are as follows (Timoshenko and Gere, 1961; Xue, 2002):

$$\frac{d^2y_1}{d\theta^2}+k_1^2y_1=0 \quad ;-\beta\le\theta\le\beta \tag{1}$$

$$\frac{d^2y_2}{d\theta^2}+k_2^2y_2=0 \quad ;\ \beta\le\theta\le 2\beta,-\beta\le\theta\le-2\beta \tag{2}$$

$$\frac{d^2y_3}{d\theta^2}+k_3^2y_3=0 \quad ;\ 2\beta\le\theta\le 3\beta,-2\beta\le\theta\le-3\beta \tag{3}$$

$$\frac{d^2y_4}{d\theta^2}+k_4^2y_4=0 \quad ;\ 3\beta\le\theta\le 4\beta,-3\beta\le\theta\le-4\beta \tag{4}$$

$$\frac{d^2y_5}{d\theta^2}+k_5^2y_5=0 \quad ;\ 4\beta\le\theta\le 5\beta,-4\beta\le\theta\le-5\beta \tag{5}$$

$$\frac{d^2y_6}{d\theta^2}+k_6^2y_6=0 \quad ;\ 5\beta\le\theta\le 2\pi-5\beta \tag{6}$$

where y is the radial deflection of the non-uniform ring, β is the angular extent and k_1 to k_6 are buckling load parameters for regions 1, 2, 3, 4, 5 and 6, respectively.

The buckling load parameters may be defined as:

$$k_i^2=1+\frac{12(1-\upsilon^2)pR^3}{Et_i^3} \tag{7}$$

where i = 1 to 6, representing the stepped region,

E is the modulus of elasticity,

υ is Poisson's ratio,

P is the external hydrostatic pressure and

t_i is the thickness for regions 1, 2, 3, 4, 5 and 6, respectively.

The general solutions of Eqs. (1) to (6) in trigonometric form are:

$$y_1(\theta)=A_1\sin k_1\theta+A_2\sin k_1\theta \quad \text{with} \quad -\beta\le\theta\le\beta \tag{8}$$

$$y_2(\theta)=B_1\sin k_2\theta+B_2\sin k_2\theta \quad \text{with} \quad \beta\le\theta\le 2\beta,\ -\beta\le\theta\le-2\beta \tag{9}$$

$$y_3(\theta)=C_1\sin k_3\theta+C_2\sin k_3\theta \quad \text{with} \quad 2\beta\le\theta\le 3\beta,\ -2\beta\le\theta\le-3\beta \tag{10}$$

$$y_4(\theta)=D_1\sin k_4\theta+D_2\sin k_4\theta \quad \text{with} \quad 3\beta\le\theta\le 4\beta,\ -3\beta\le\theta\le-4\beta \tag{11}$$

$$y_5(\theta)=E_1\sin k_5\theta+E_2\sin k_5\theta \quad \text{with} \quad 4\beta\le\theta\le 5\beta,\ -4\beta\le\theta\le-5\beta \tag{12}$$

$$y_6(\theta)=F_1\sin k_6\theta+F_2\sin k_6\theta \quad \text{with} \quad 5\beta\le\theta\le 2\pi-5\beta \tag{13}$$

where A_1, A_2, B_1, B_2, C_1, C_2, D_1, D_2, E_1, E_2, F_1 and F_2 are constants of integration to be determined by applying both boundary and continuity conditions.

BOUNDARY AND CONTINUITY CONDITIONS

The boundary and continuity conditions for both symmetric and anti-symmetric buckling modes differ from each other. The symmetric and anti-symmetric modes require that the deflections and the slopes are all continuous at boundaries $\theta=\beta$, $\theta=2\beta$, $\theta=3\beta$, $\theta=4\beta$, $\theta=5\beta$ and $\theta=2\pi$-5β, respectively. Now, for the symmetric buckling mode, the slope ($dy/d\theta$) is equal to zero at $\theta=0$ and $\theta=\pi$ and for the anti-symmetric buckling mode the bending moment ($d^2y/d\theta^2$) is equal to zero at $\theta=0$ and $\theta=\pi$.

EXACT EIGENVALUE SOLUTION FOR SYMMETRIC AND ANTI-SYMMETRIC BUCKLING MODES

The real critical buckling pressure and mode of the non-uniform ring can be obtained as the smallest value for the buckling pressure from separate solution of symmetric and anti-symmetric mode as coming next.

Exact Symmetric Eigenvalue Solution

The twelve boundary and continuity conditions needed to determine the twelve integration constants for the symmetric mode can be written as:

$$\frac{dy_1}{d\theta} = 0 \text{ ; at } \quad \theta = 0 \tag{14}$$

$$y_1 = y_2 \text{ , and } \frac{dy_1}{d\theta} = \frac{dy_2}{d\theta} \text{ ; at } \quad \theta = \beta \tag{15}$$

$$y_2 = y_3 \text{ , and } \frac{dy_2}{d\theta} = \frac{dy_3}{d\theta} \text{ ; at } \quad \theta = 2\beta \tag{16}$$

$$y_3 = y_4 \text{ , and } \frac{dy_3}{d\theta} = \frac{dy_4}{d\theta} \text{ ; at } \quad \theta = 3\beta \tag{17}$$

$$y_4 = y_5 \text{ , and } \frac{dy_4}{d\theta} = \frac{dy_5}{d\theta} \text{ ; at } \quad \theta = 4\beta \tag{18}$$

$$y_5 = y_6 \text{ , and } \frac{dy_5}{d\theta} = \frac{dy_6}{d\theta} \text{ ; at } \quad \theta = 5\beta \tag{19}$$

$$\frac{dy_6}{d\theta} = 0 \text{ ; at } \quad \theta = \pi \tag{20}$$

By applying the boundary and continuity conditions of Eqs. (14) to (20) into Eqs. (1) to (13), a system of twelve simultaneous equations containing trigonometric functions can be obtained and gathered in a banded matrix symbolic form which can be summarized as:

$$[K_s]\{A\} = \{0\} \tag{21}$$

For a non-trivial solution of Eq. (21) we must have

$$|K_s| = 0 \tag{22}$$

After some mathematical and trigonometric substitutions using the MATHEMATICA program (MATHEMATICA, Version 5.0, 2003), the transcendental equation for the symmetric case is obtained to be:

$$\tan[(\pi - 5\beta)k_6] = \frac{f_1(k_1, k_2, k_3, k_4, k_5, k_6, \beta)}{g_1(k_1, k_2, k_3, k_4, k_5, k_6, \beta)} \tag{23}$$

where

$$\begin{aligned} f_1 = k_5 \big[& k_1 k_2 k_3 k_4 T(\bar{k}_1) + k_2^2 k_3 k_4 T(\bar{k}_2) + k_2 k_3^2 k_4 T(\bar{k}_3) + k_2 k_3 k_4^2 T(\bar{k}_4) + k_2 k_3 k_4 k_5 T(\bar{k}_5) - \\ & k_1 k_3^2 k_4 T(\bar{k}_1) T(\bar{k}_2) T(\bar{k}_3) - k_1 k_3 k_4^2 T(\bar{k}_1) T(\bar{k}_2)(k_4) - k_1 k_2 k_4^2 T(\bar{k}_1) T(\bar{k}_3) T(\bar{k}_4) - \\ & k_2^2 k_4^2 T(\bar{k}_2) T(\bar{k}_3) T(\bar{k}_4) - k_1 k_3 k_4 k_5 T(\bar{k}_1) T(\bar{k}_2) T(\bar{k}_5) - k_1 k_2 k_4 k_5 T(\bar{k}_1) T(\bar{k}_3) T(\bar{k}_5) - \\ & k_2^2 k_4 k_5 T(\bar{k}_2) T(\bar{k}_3) T(\bar{k}_5) - k_1 k_2 k_3 k_5 T(\bar{k}_1) T(\bar{k}_4) T(\bar{k}_5) - k_2^2 k_3 k_5 T(\bar{k}_2) T(\bar{k}_4) T(\bar{k}_5) - \\ & k_2 k_3^2 k_5 T(\bar{k}_3) T(\bar{k}_4) T(\bar{k}_5) - k_1 k_3^2 k_5 T(\bar{k}_1) T(\bar{k}_2) T(\bar{k}_3) T(\bar{k}_4) T(\bar{k}_5) \big] \end{aligned} \tag{24}$$

and

$$\begin{aligned} g_1 = k_6 \big[& k_2 k_3 k_4 k_5 - k_1 k_3 k_4 k_5 T(\bar{k}_1) T(\bar{k}_2) - k_1 k_2 k_4 k_5 T(\bar{k}_1) T(\bar{k}_3) - \\ & k_2^2 k_4 k_5 T(\bar{k}_2) T(\bar{k}_3) - k_1 k_2 k_3 k_5 T(\bar{k}_1) T(\bar{k}_4) - k_2^2 k_3 k_5 T(\bar{k}_2) T(\bar{k}_4) - \\ & k_2 k_3^2 k_5 T(\bar{k}_3) T(\bar{k}_4) + k_1 k_3^2 k_5 T(\bar{k}_1) T(\bar{k}_2) T(\bar{k}_3) T(\bar{k}_4) - k_1 k_2 k_3 k_4 T(\bar{k}_1) T(\bar{k}_5) - \\ & k_2^2 k_3 k_4 T(\bar{k}_2) T(\bar{k}_5) - k_2 k_3^2 k_4 (k_3) T(\bar{k}_5) + k_1 k_3^2 k_4 T(\bar{k}_1) T(\bar{k}_2) T(\bar{k}_3) T(\bar{k}_5) - \\ & k_2 k_3 k_4^2 T(\bar{k}_4) T(\bar{k}_5) + k_1 k_3 k_4^2 T(\bar{k}_1) T(\bar{k}_2) T(\bar{k}_4) T(\bar{k}_5) + \\ & k_1 k_2 k_4^2 T(\bar{k}_1) T(\bar{k}_3) T(\bar{k}_4) T(\bar{k}_5) + k_2^2 k_4^2 T(\bar{k}_2) T(\bar{k}_3) T(\bar{k}_4) T(\bar{k}_5) \big] \end{aligned} \tag{25}$$

with

$$T(\bar{k}_1) = \tan(\beta k_1);\ T(\bar{k}_2) = \tan(\beta k_2); T(\bar{k}_3) = \tan(\beta k_3); T(\bar{k}_4) = \tan(\beta k_4); T(\bar{k}_5) = \tan(\beta k_5)$$

Exact Anti-symmetric Eigenvalue Solution

The twelve boundaries and continuity conditions needed to determine the twelve constants of integration for the anti-symmetric mode can be written as:

$$\frac{d^2y_1}{d\theta^2}=0 \text{ ; at } \quad \theta=0 \tag{26}$$

$$y_1=y_2 \text{ , and } \frac{dy_1}{d\theta}=\frac{dy_2}{d\theta} \text{ ; at } \quad \theta=\beta \tag{27}$$

$$y_2=y_3 \text{ , and } \frac{dy_2}{d\theta}=\frac{dy_3}{d\theta} \text{ ; at } \quad \theta=2\beta \tag{28}$$

$$y_3=y_4 \text{ , and } \frac{dy_3}{d\theta}=\frac{dy_4}{d\theta} \text{ ; at } \quad \theta=3\beta \tag{29}$$

$$y_4=y_5 \text{ , and } \frac{dy_4}{d\theta}=\frac{dy_5}{d\theta} \text{ ; at } \quad \theta=4\beta \tag{30}$$

$$y_5=y_6 \text{ , and } \frac{dy_5}{d\theta}=\frac{dy_6}{d\theta} \text{ ; at } \quad \theta=5\beta \tag{31}$$

$$\frac{d^2y_6}{d\theta^2}=0 \text{ ; at } \quad \theta=\pi \tag{32}$$

By a similar procedure to that in the symmetric mode case, the Eigenvalue solution leads to a transcendental equation for the anti-symmetric mode case as:

$$\tan[(\pi-5\beta)k_6]=\frac{f_2(k_1,k_2,k_3,k_4,k_5,k_6,\beta)}{g_2(k_1,k_2,k_3,k_4,k_5,k_6,\beta)} \tag{33}$$

where f_2 and g_2 can be defined in a similar manner for these of the symmetric mode case as:

$$\begin{aligned} f_2 = k_6\big[&k_2k_3k_4k_5T(\bar{k}_1)+k_1k_3k_4k_5T(\bar{k}_2)+k_1k_2k_4k_5T(\bar{k}_3)+k_1k_2k_3k_5T(\bar{k}_4)+\\ &k_1k_2k_3k_4T(\bar{k}_5)-k_2^2k_4k_5T(\bar{k}_1)T(\bar{k}_2)T(\bar{k}_3)-k_2^2k_3k_5T(\bar{k}_1)T(\bar{k}_2)T(\bar{k}_4)-\\ &k_2k_3^2k_5T(\bar{k}_1)T(\bar{k}_3)T(\bar{k}_4)-k_1k_3^2k_5T(\bar{k}_2)T(\bar{k}_3)T(\bar{k}_4)-k_2^2k_3k_4k_5T(\bar{k}_1)T(\bar{k}_2)T(\bar{k}_5)-\\ &k_2k_3^2k_4T(\bar{k}_1)T(\bar{k}_3)T(\bar{k}_5)-k_1k_3^2k_4T(\bar{k}_2)T(\bar{k}_3)T(\bar{k}_5)-k_2k_3k_4^2T(\bar{k}_1)T(\bar{k}_4)T(\bar{k}_5)-\\ &k_1k_3k_4^2T(\bar{k}_2)T(\bar{k}_4)T(\bar{k}_5)-k_1k_2k_4^2T(\bar{k}_3)T(\bar{k}_4)T(\bar{k}_5)-k_2^2k_4^2T(\bar{k}_1)T(\bar{k}_2)T(\bar{k}_3)T(\bar{k}_4)T(\bar{k}_5)\big] \end{aligned} \tag{34}$$

$$\begin{aligned} g_2 = k_5\big[&k_1k_2k_3k_4-k_2^2k_3k_4T(\bar{k}_1)T(\bar{k}_2)-k_2k_3^2k_4T(\bar{k}_1)T(\bar{k}_3)-k_1k_3^2k_4T(\bar{k}_2)T(\bar{k}_3)-\\ &k_2k_3k_4^2T(\bar{k}_1)T(\bar{k}_4)-k_1k_3k_4^2T(\bar{k}_2)T(\bar{k}_4)-k_1k_2k_4^2T(\bar{k}_3)T(\bar{k}_4)+\\ &k_2^2k_4^2T(\bar{k}_1)T(\bar{k}_2)T(\bar{k}_3)T(\bar{k}_4)-k_2k_3k_4k_5T(\bar{k}_1)T(\bar{k}_5)-k_1k_3k_4k_5T(\bar{k}_2)T(\bar{k}_5)-\\ &k_1k_2k_4k_5T(\bar{k}_3)T(\bar{k}_5)+k_2^2k_4k_5T(\bar{k}_1)T(\bar{k}_2)T(\bar{k}_3)T(\bar{k}_5)-k_1k_2k_3k_5T(\bar{k}_4)T(\bar{k}_5)+\\ &k_2^2k_3k_5T(\bar{k}_1)T(\bar{k}_2)T(\bar{k}_4)T(\bar{k}_5)+k_2k_3^3k_5T(\bar{k}_1)T(\bar{k}_3)T(\bar{k}_4)T(\bar{k}_5)+\\ &k_1k_3^2k_5T(\bar{k}_2)T(\bar{k}_3)T(\bar{k}_4)T(\bar{k}_5)\big] \end{aligned} \tag{35}$$

with

$$T(\bar{k}_1)=\tan(\beta k_1);\ T(\bar{k}_2)=\tan(\beta k_2);\ T(\bar{k}_3)=\tan(\beta k_3);\ T(\bar{k}_4)=\tan(\beta k_4);\ T(\bar{k}_5)=\tan(\beta k_5)$$

COMPUTER PROGRAM

The bisection method was used to solve Eqs. (23) and (33) to determine the critical buckling pressures for symmetrical and anti-symmetrical modes, respectively. Accordingly, a computer program using QBasic language was coded and prepared to solve the problem under consideration.

This non-uniform ring problem was generalized by selecting the variables to be the angular extent β and the ratio of the thickness in the corroded region t_1 with respect to the thickness in the un-corroded region t_6 (i.e., t_1/t_6). In order to obtain the other thicknesses in the corroded regions t_2 to t_5, one may create relationships between these thicknesses with respect to t_6. Practically, to obtain these relationships in the corroded regions a general continuous function may be assumed. This function can be any polynomial up to the fifth degree. In this study, and for simplicity, a parabolic variation in the thickness of the corroded portion was adopted as shown in Fig. 2 where the un-corroded portion had a thickness equal to t. Herein, the thickness in the corroded portion varies by the parabolic function $t(\theta)$

and ranges from a minimum value t_m to a maximum value t and having an angular extent equal to ω. The parabolic function may be represented as:

$$t(\theta) = (t - t_m)\frac{\theta^2}{\omega^2} + t_m \tag{36}$$

To simulate the practical selected non-uniform thin shell with the parabolic variation (Fig. 2) to the stepped non-uniform ring (Fig. 1), the angular extent is divided into five equal parts each having an angular extent of β (i.e. $\theta = 5\beta$). To obtain the equivalent thicknesses in the corroded regions t_2 to t_5 in Fig.1, one may use Eq.(36) along with the mean moment of inertia within each part. As a representative example and for the region where θ varies from zero to β, the thickness t_1 in corroded region 1 shown in Fig. 1 is obtained as:

$$\text{at } \theta = 0: \; t(0) = t_m; \qquad I(0) = \frac{t_m^3}{12} \tag{37}$$

$$\text{at } \theta = \beta: \; t(\beta) = \frac{(t - t_m)}{25} + t_m; \; I(\beta) = \frac{1}{12}\left[\frac{(t - t_m)}{25} + t_m\right]^3 \tag{38}$$

Then the thickness t_1 can be obtained from the mean moment of inertia in the region where θ varies from zero to β as:

$$t_1 = t\left[\frac{t_m^3}{2t^3} + \frac{1}{2}\left[\frac{1}{25} + \frac{t_m}{24t}\right]^3\right]^{\frac{1}{3}} \tag{39}$$

It can be noted that the thickness t_1 is a function of two variables that are the un-corroded thickness t and the ratio of minimum thickness with respect to t (i.e. t_m/t). Similarly, the other thicknesses in the corroded regions t_2 to t_5 can be written as functions of the former two variables.

BUCKLING ANALYSIS OF THE NON-UNIFORM RING USING ABAQUS

To check the accuracy and robustness of the present analytical solution, a buckling analysis using the finite element package ABAQUS (ABAQUS/Standard User's Manual, 2003) was performed. The two-noded Euler type uniform beam element B21 is used to model the non-uniform stepped ring shown in Fig.1. Each corroded region was divided into 60 beam elements and the un-corroded region into 300 elements. In order to get the actual behavior of the ring under external hydrostatic pressure (symmetrical or antisymmetrical buckling modes), the upper node (i.e., at $\theta = \pi$) was so that horizontal and vertical displacements and rotation about the global z-axis (i.e., u_x, u_y and θ_z) were equal to zero. The reason for selecting one node to be the constrained was to allow the ring to choose its real buckling mode. It should be noted that selecting further nodes to be constrained will result in higher buckling modes.

NUMERICAL EXAMPLES AND DISCUSSIONS

A non-uniform long ring made from steel was considered with the following properties: E = 200000 MPa; ν = 0.3; R = 1000 mm; un-corroded thickness, t = t_6 = 20 mm. For the purpose of analysis and generalization, the critical buckling pressure of a non-uniform ring was normalized with respect to the elastic critical buckling pressure (P_e) for a uniform ring having uniform thickness equal to t_6 as follows:

$$\lambda_c = \frac{P_{cr}}{P_e} \tag{40}$$

where

$$P_e = \frac{Et_6^3}{12(1-\upsilon^2)R^3} \tag{41}$$

Fig. 3 shows the variation of the critical buckling pressure parameter λ_c *versus* the angular extent β (in degrees) for different (t_m/t) ratios. It can be seen from Fig. 3 that the buckling pressure decreases with increasing the angular extent β. A sudden decrease in the buckling pressure for small values of (t_m/t) ratio and the angular extent β (for $\beta \leq 10^o$ and $(t_m/t) \leq 0.3$) can also be seen. The analytical results shown in Fig. 3 are in good agreement with the finite element results obtained by ABAQUS. However, an insignificant discrepancy between ABAQUS and the analytical results has been noticed at

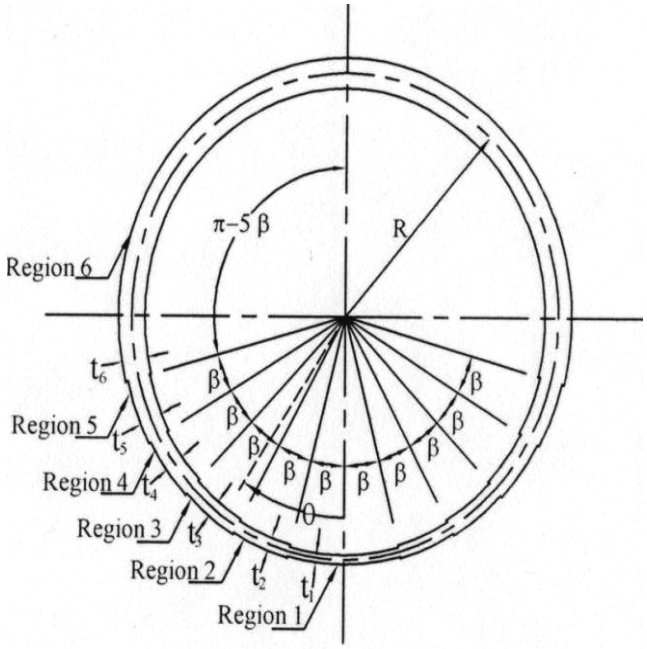

Figure (1): Cross-section of stepped non-uniform ring

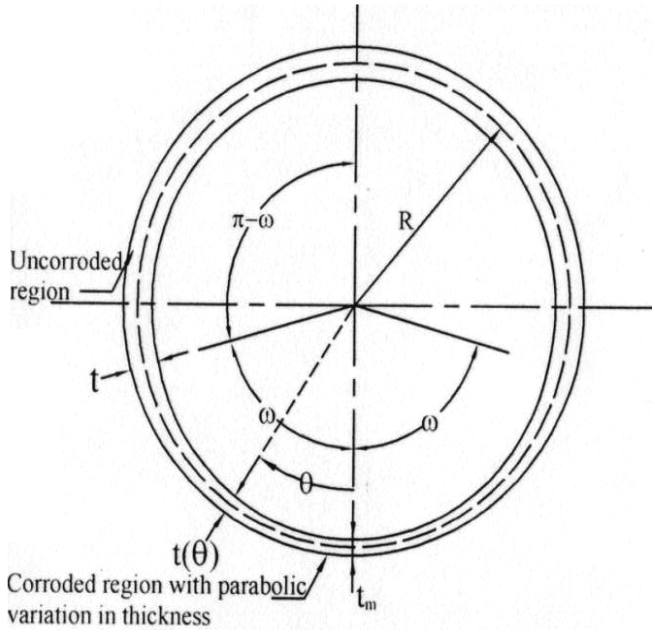

Figure (2): Cross-section of non-uniform ring with parabolic variation in thickness of corroded region

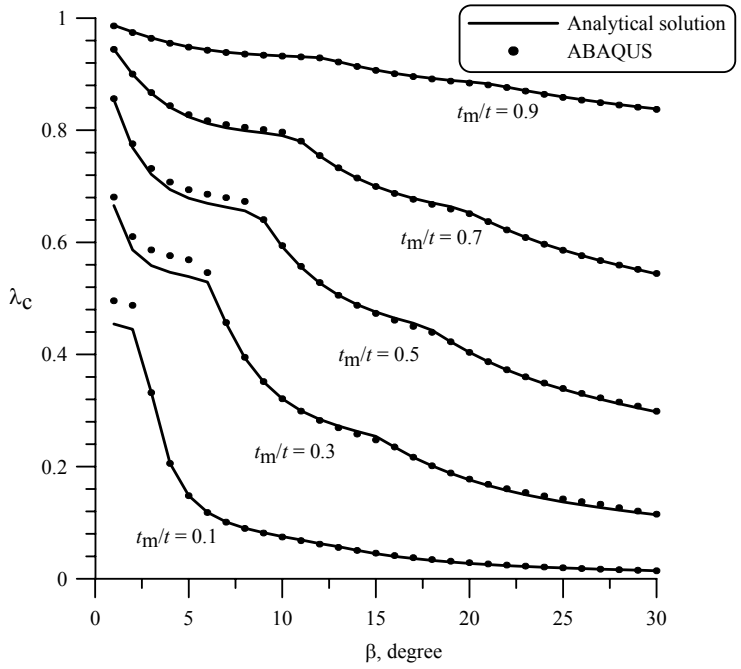

Figure (3): Variation of the critical buckling pressure parameter with β for different t_m/t ratios

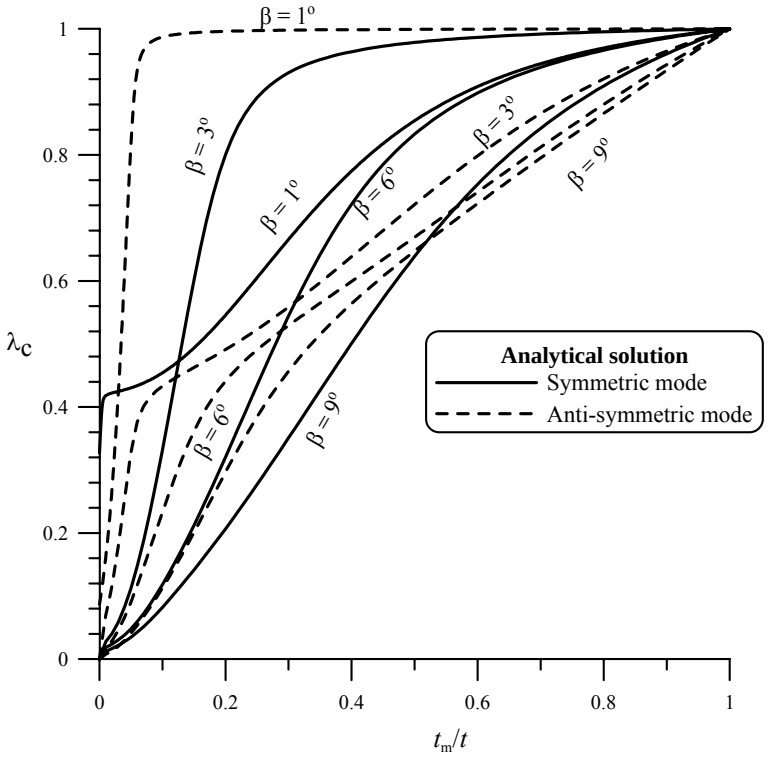

Figure (4): Variation of the critical buckling pressure parameter with t_m/t ratio and for β = 1°, 3° and 6°

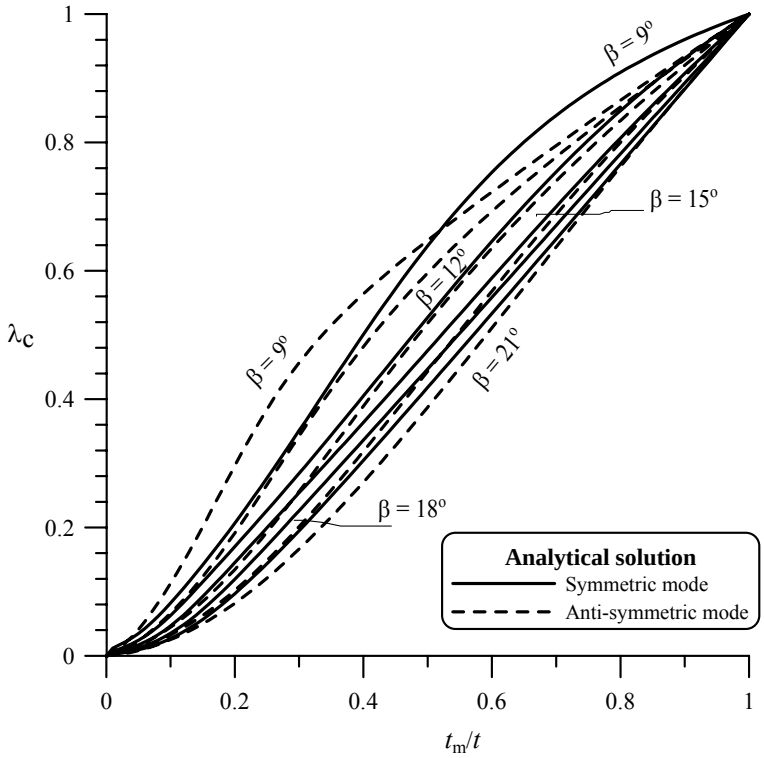

Figure (5): Variation of the critical buckling pressure parameter with t_m/t ratio and for β = 9°, 12°, 15°, 18° and 21°

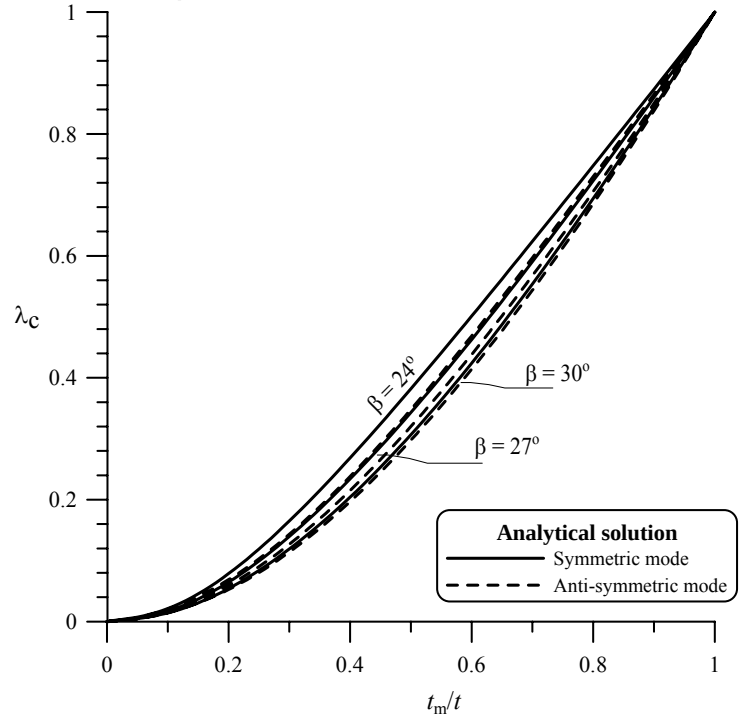

Figure (6): Variation of the critical buckling pressure parameter with t_m/t ratio and for β = 24°, 27° and 30°

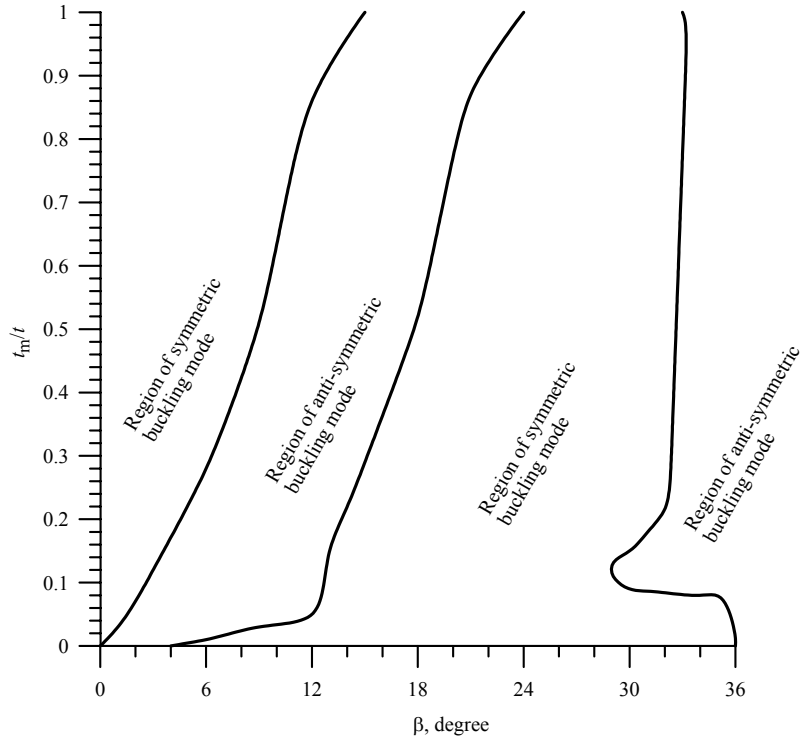

Figure (7): Regions of symmetric and anti-symmetric buckling modes as a function of t_m/t ratio and for different β values

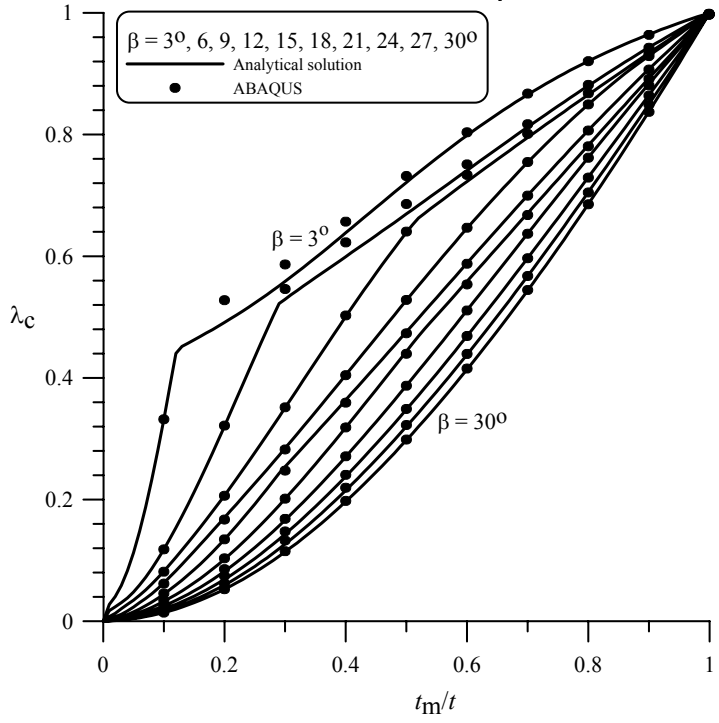

Figure (8): Variation of the critical buckling pressure parameter with t_m/t ratio and for different β values

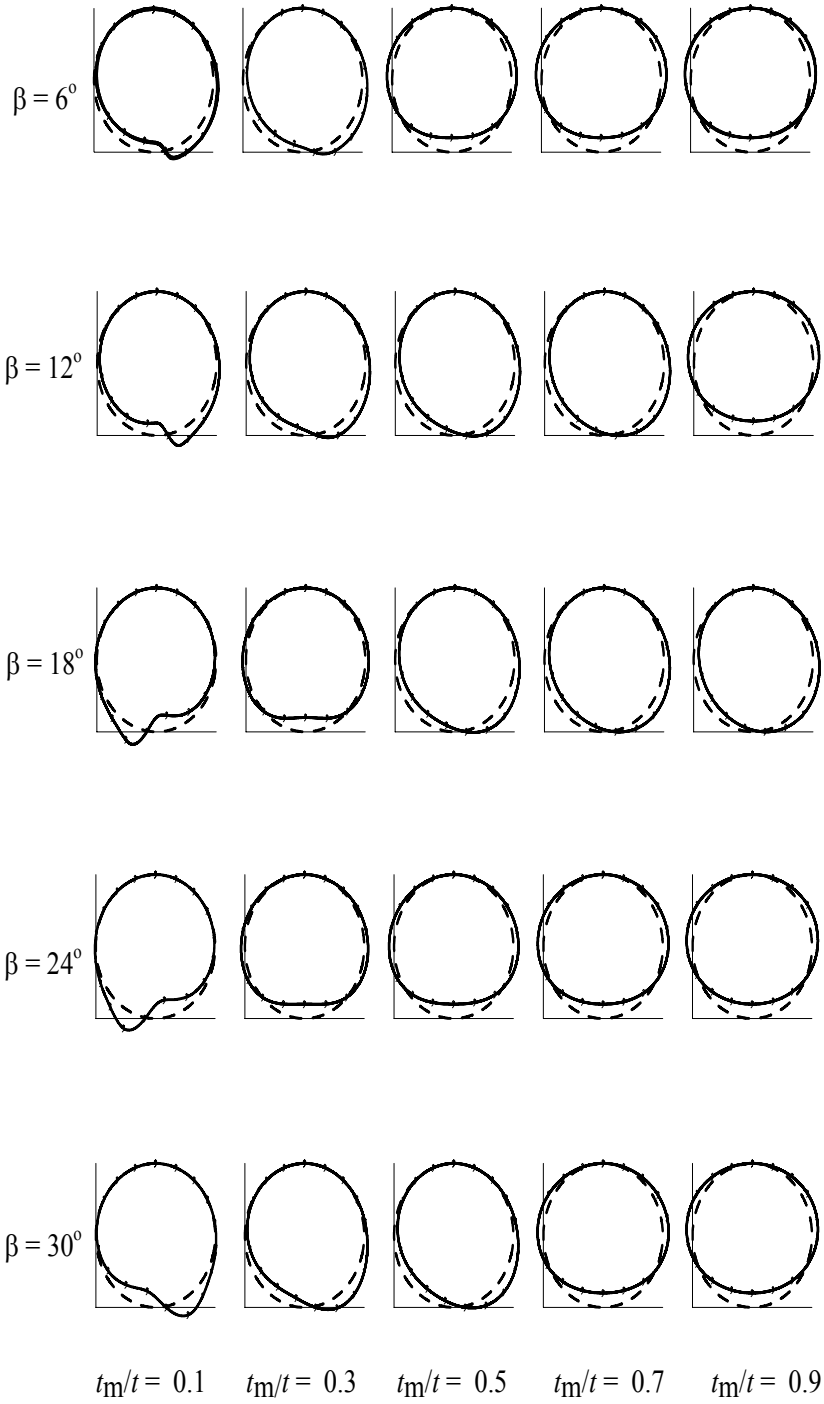

Figure (9): Buckling mode shapes for different t_m/t ratio and different β values

very low values of β. This is because of using uniform beam elements with constant thickness for each corroded region in ABAQUS model to ideally match the analytical problem using multi stepped type model. Figs. 4 to 6

show the variation of the critical buckling pressure parameter with different (t_m/t) ratios and different β values ($\beta = 1^o$, 3, 6, 9, 12, 15, 18, 21, 24, 27 and 30^o). Figs. 4 to 6 show two separate cases of symmetrical and anti-symmetrical buckling modes as discussed earlier. To determine the critical buckling pressure, the smallest value for each case of symmetric and anti-symmetric modes is selected. Thus, one may recognize that the occurrence of symmetrical and anti-symmetrical buckling modes depends upon the (t_m/t) ratio and β values. For example, it was observed that the critical buckling pressure parameter for an anti-symmetrical mode is less than that for the symmetrical mode when $\beta = 6^o$ and when $0 \leq (t_m/t) \leq 0.29$. Therefore, the buckling pressure in this range causes an anti-symmetrical buckling mode. Also, one may note that as the angular extent β increases (i.e. $\beta > 18^o$), values of the of critical buckling pressures for both symmetrical and anti-symmetrical buckling modes are close to each other and the buckling pressures for symmetrical buckling modes are always dominant.

Fig. 7 shows regions of symmetric and anti-symmetric buckling modes as functions of β and (t_m/t) ratios. These regions were obtained by investigating the results shown in Figs. 4 to 6 using the MATHEMATICA program. For each region given in Fig. 7, the values of the buckling pressures obtained from the symmetrical modes were set equal to those given in the anti-symmetrical modes. The first curve (from the left) shown in Fig. 7 represents the buckling modes at the point of change from symmetrical to anti-symmetrical modes. The second curve represents buckling modes at the point of change from anti-symmetrical to symmetrical modes and *vice versa* for the third and fourth curves.

Fig. 8 shows the variation of the critical buckling pressure parameter with (t_m/t) ratio for different β values. Again, the analytical results shown in Fig. 8 are in good agreement with the finite element results by ABAQUS. Fig. 9 shows some of the buckling modes which are a consequence of the solution given in Fig. 7. Also, Fig. 9 shows a good agreement between present analytical buckling modes and these obtained by ABAQUS. The sequence of changes in buckling modes shown in Fig. 9 coincides very well with these shown in Fig. 7.

CONCLUDING REMARKS

Exact analytical solution has been derived for determing the elastic critical buckling pressures and mode shapes of long cylindrical steel shells considering symmetrical and anti-symmetrical mode cases. The long cylindrical shell has been modelled as a non-uniform multi "stepped-type" ring. The multi stepped type of the corroded regions is able to capture many polynomial curves of the corroded regions.

The study shows that buckling loads and modes depend on the corrosion angular extent β and the corroded to un-corroded thicknesses ratio. The actual buckling mode for both symmetrical and anti-symmetrical cases is obtained and found to depend on the angular extent β and the corroded to un-corroded thicknesses ratio(t_m/t) ratio. A comparison study has been made with the finite element package ABAQUS and the results showed close agreement. However, future work using tapered beam elements may be carried out to see how good the stepped approximation is to the true model.

REFERENCES

ABAQUS/Standard User's Manual. 2003. Version 6.4, Hibbitt, Karlsson and Sorensen, Inc.

Bai, Y. and Hauch, S. 1998. Analytical Collapse of Corroded Pipes, *Proceedings of the 8th International Conference on Offshore and Polar Engineering*, Montreal, Canada, 24-29 May,182-190.

Bai, Y., Hauch, S. and Jenses, J.C. 1999. Local Buckling and Plastic Collapse of Corroded Pipes with Yield

Anisotropy, *Proceedings of the 9th International Offshore and Polar Engineering Conference*, Golden, Co, May, 74-81.

Fatt, Hoo M.S. 1999. Elastic-Plastic Collapse of Non-Uniform Cylindrical Shells Subjected to Uniform External Pressure, *Thin Walled Struct.,* 35:117-154.

MATHEMATICA, Version 5.0. 2003. Wolfram Research, Inc.

Pinna, R. and Ronalds, B.F. 2000. Hydrostatic Buckling of Shells with Various Boundary Conditions, *J. Constr. Steel Research*, 56 (1): 1-16.

Timoshenko, S.V. and Gere, J.M. 1961. Theory of Elastic Stability, McGraw-Hill, NY.

Vodenitcharova, T. and Ansourian, P. 1996. Buckling of Circular Cylindrical Shells Subject to Uniform Lateral Pressure, *Engineering Structure*, 18 (8): 604-614.

Xue, J. and Fatt, Hoo M.S. 2002. Buckling of a Non-Uniform, Long Cylindrical Shell Subjected to External Hydrostatic Pressure, *Engineering Structure*, 24: 1027-1034.

Xue, J. 2002. *Structural Failure of Non-Uniform, Infinitely Long Cylindrical Shells Subjected to Uniform External Pressure*. Doctoral Dissertation, The University of Akron,USA.

Xue, J. and Fatt, Hoo M.S. 2005. Symmetric and Anti-symmetric Buckle Propagation Modes in Subsea Corroded Pipelines, *Marine Structures*, 18: 43-61.